

The air density varies with the distance ( $x$ ) from the mirror points as  $N_0 e^{-x/h}$  where  $N_0$  is the air density and  $h$  the scale height at the mirror points, respectively. From the above equations we obtain

$$\dot{\gamma} = -3.10^{-8} N_0 Z \exp\left(-\frac{3c^2}{4r_0 h} t^2\right) \quad (11)$$

Integration of this equation from zero to infinity shall yield the energy loss along one trajectory from the reflection point to the equator. Then considering the oscillation time we derive the average energy loss, namely

$$\langle \dot{\gamma} \rangle = \frac{3.10^{-8} N_0 Z}{\psi} \sqrt{\frac{h}{r_0}} \quad \text{rmu/day} \quad (12)$$

where  $(r_0\psi)$  is the length of the magnetic line from the mirror point to the equator. The rate of change of the scattering angle ( $\theta^2$ ) is a function of  $\dot{\gamma}$ , just evaluated, and a function of  $\gamma^2$ . The value of  $\gamma$  is reduced from Coulomb scattering and Schwinger radiation loss. However, the contribution from Schwinger radiation is small for  $N_0$  more than  $10^6$  atoms per  $\text{cm}^3$ . Equations (6), (7), and (12) yield

$$\dot{x} \equiv \dot{R} = -\frac{10^{-8} Z(Z+1)N_0}{\psi\gamma^2} r_0 \sqrt{\frac{h}{r_0}} \quad (13)$$

As the mirror points move downward the air density increases. Consequently at a distance  $x$  (downward) from the initial mirror point the downward velocity is

$$\dot{x} = -\frac{10^{-8} Z(Z+1)}{\psi\gamma^2} N_0 e^{-x/h} r_0 \sqrt{\frac{h}{r_0}} \quad (14)$$

In the case of electrons of a few Mev energy, the loss of the electrons is due more to scattering than to energy loss, namely, the mirror points move downward one scale height without appreciable energy loss. In this case equation (14) yields upon integration

$$T = 1.7 \cdot 10^6 \frac{\psi\gamma^2}{N_0} \sqrt{\frac{h}{r_0}} \quad \text{days.} \quad (15)$$

\* Work was performed under auspices of the U. S. Atomic Energy Commission.

<sup>1</sup> Van Allen, James A., Carl E. McIlwain, and George H. Ludwig, these PROCEEDINGS, 45, 1152-1171 (1959).

<sup>2</sup> Northrop, T., and E. Teller, Univ. of Calif. Rad. Lab. Report, UCRL-5615 (to be published).

### SATELLITE OBSERVATIONS OF ELECTRONS ARTIFICIALLY INJECTED INTO THE GEOMAGNETIC FIELD

BY JAMES A. VAN ALLEN, CARL E. MCILWAIN, AND GEORGE H. LUDWIG

DEPARTMENT OF PHYSICS, STATE UNIVERSITY OF IOWA

Following our discovery with Explorer I (Satellite 1958 Alpha) and with Explorer III (Satellite 1958 Gamma) that there were very great intensities of charged particles trapped in the geomagnetic field,<sup>1</sup> we undertook to make arrangements for a further satellite flight of equipment of greater discrimination and much greater

dynamic range for the purpose of detailed study of the properties of the radiation and of its spatial distribution. The progress of such arrangements was greatly aided by Richard W. Porter, chairman of the Technical Panel for the Earth Satellite Program of the U.S. National Committee for the International Geophysical Year, and by Herbert York, then chief scientist of the Advanced Research Projects Agency of the Department of Defense.

In October, 1957, Nicholas C. Christofilos of the Lawrence Radiation Laboratories of the University of California at Livermore had proposed in an unpublished memorandum that many observable geophysical effects could be produced by an atomic detonation at high altitude above the earth in the tenuous upper atmosphere. Of the various effects contemplated one of the most interesting promised to be the temporary trapping of high energy electrons at high altitudes in the geomagnetic field. Such electrons result from the radioactive decay of fission fragments and, less importantly, of neutrons.

A subsequently organized study group carried out more detailed estimates of the various effects to be expected and concluded that the proposed experiments (later named "Argus" experiments) were indeed feasible. This study group, led by W. K. H. Panofsky, also concluded that satellite observations would be of great value.

Meanwhile, the discovery of the existence of the natural, trapped radiation served as an over-all validation of the Argus proposal in that it showed that a high intensity of charged particles can indeed be trapped in the geomagnetic field. And to the I.G.Y. workers at the State University of Iowa and elsewhere it was clear that the artificial, impulsive injection of known particles along a known line of force, at a known time, would be a powerful technique for elucidating many of the uncertain aspects of the dynamics of geomagnetic trapping.

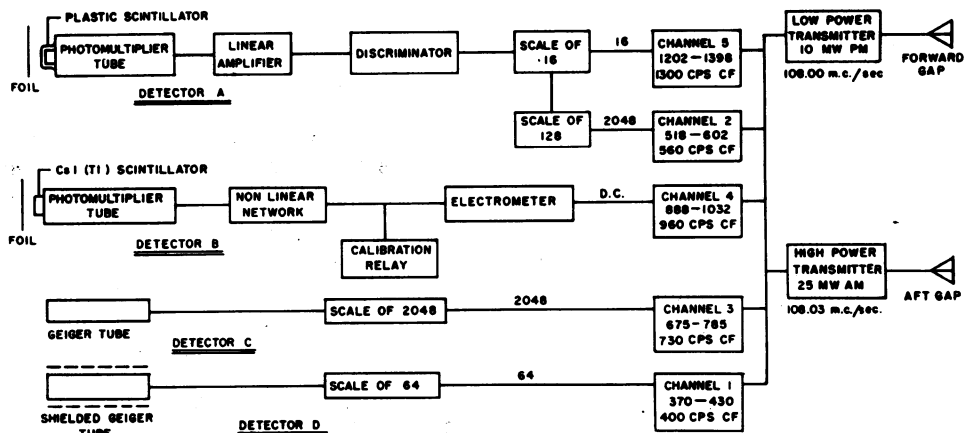
After a series of conferences, the Advanced Research Projects Agency agreed to provide, among other things, two Jupiter C satellite vehicles for the joint I.G.Y.-Argus undertaking.

Design, development, construction, and calibration of the detectors, associated electronics, etc., were accomplished within the Department of Physics of the State University of Iowa (S.U.I.). The apparatus was designed around the two-fold purpose of further, detailed study of the natural radiation and of detection and quantitative study of artificially injected electrons from the Argus experiments. Final environmental tests and over-all specifications of the flight payloads were in the hands of the Army Ballistic Missile Agency (ABMA), as were the supply of payload shells, thermal design of the shells and, of course, many other essential aspects of the flight operations. Telemetry transmitters and other electronic components were provided by the Jet Propulsion Laboratory (J.P.L.), by Project Vanguard, and by the Army Signal Engineering and Development Laboratory.

Four flight payloads were built, fully calibrated and subjected to the full gamut of environmental tests. One payload was flown in Explorer IV, which entered a  $51^\circ$  inclination orbit successfully at 1506 UT on July 26, 1958, thus earning the astronomical designation Satellite 1958 Epsilon. The apparatus performed in all respects fully up to expectations, though the lifetime of its batteries was somewhat shorter than expected.

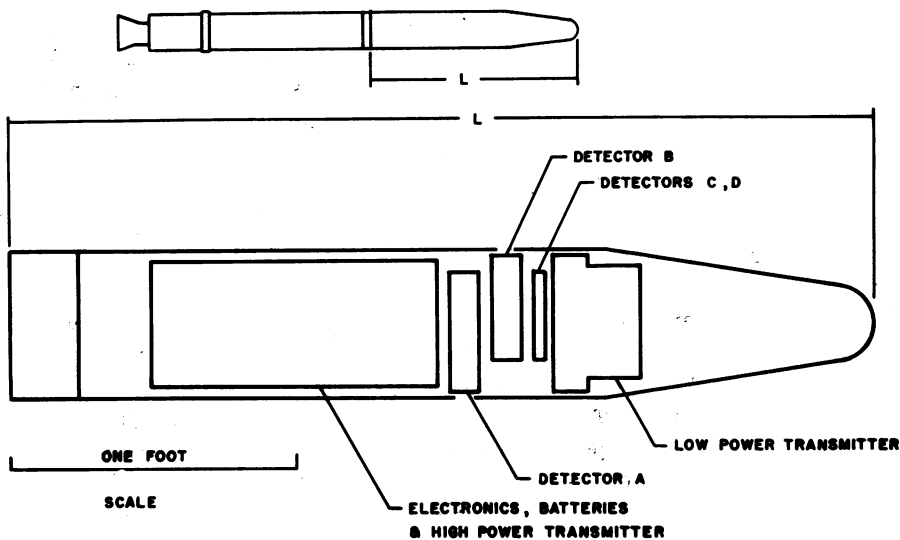
A second payload was flown on Explorer V, launched on August 24, 1958. This

rocket failed to go into orbit. However, the on-board apparatus functioned properly during its brief flight.



SATELLITE 1958 EPSILON — STATE UNIVERSITY OF IOWA

Fig. 1.—Block diagram of detectors and associated circuitry of Explorer IV.



PAYLOAD CONFIGURATION — SATELLITE 1958 EPSILON

Fig. 2.—Outline sketch of the arrangement of principal components of the payload of Explorer IV (satellite 1958 epsilon); small diagram in upper part of the figure shows appearance of the orbiting body, of which the payload was a permanent part.

A full description of the observing equipment of Explorer IV and a preliminary account of the observations of the natural radiation have been published.<sup>2</sup> For convenience of the present reader Table 1 summarizes the principal characteristics of the apparatus. Figures 1 and 2 show the circuit schematic and physical arrangement respectively.

TABLE 1  
SUMMARY OF DETECTOR CHARACTERISTICS (EXPLORER IV)  
(See Reference 2 for more complete description)

Channel	Detector	Shielding	Sensitive to:	Geometric Factor
1	Geiger-Mueller Counter (Anton 302) Cylinder approximately 7 mm $\times$ 9 mm Scaler: 64	1.2 g/cm <sup>2</sup> Fe + 1.6 g/cm <sup>2</sup> Pb (minimum)	Electrons of $E > 5$ mev; protons of $E > 40$ mev; X rays of $E > 80$ kev with low efficiency	Omnidirectional geometric factor 0.14 cm <sup>2</sup> for minimum stopping power; 0.82 cm <sup>2</sup> for penetrability greater than 7 g/cm <sup>2</sup>
2	Plastic scintillator 0.75 cm diameter, 0.18 cm thick; Pulse Detector Scaler: 16	0.14 g/cm <sup>2</sup> of aluminum over window	Electrons of $E > 580$ kev; protons of $E > 10$ mev. Axis of detector $\perp$ to payload axis X rays of $E > 300$ kev with low efficiency	0.040 cm <sup>2</sup> steradian; for minimum stopping power; 4.2 cm <sup>2</sup> steradian for penetrability greater than 5 g/cm <sup>2</sup>
3	Same as channel 1 except less shielding Scaler: 2048	1.2 g/cm <sup>2</sup> Fe (minimum)	Electrons of $E > 3$ mev; Protons of $E > 30$ mev; X rays of $E > 20$ kev with low efficiency	Omnidirectional geometric factor 0.14 cm <sup>2</sup> for min stopping power; 0.70 cm <sup>2</sup> for greater than 5 g/cm <sup>2</sup> stopping power
4	Cesium Iodide Crystal 0.76 cm diameter, 0.20 cm thick. Total energy-dc electrometer	1.0 mg/cm <sup>2</sup> of nickel and aluminum over window	Electrons of $E > 20$ kev; protons of $E > 400$ kev; x-rays Axis of detector — to payload axis	0.0235 cm <sup>2</sup> steradian for minimum stopping power 4.4 cm <sup>2</sup> steradian for penetrability greater than 5 g/cm <sup>2</sup>
5	Same as 2 except Scaler: 2048			

Reference 2 should be consulted for further experimental details as well as for discussion of interpretative aspects.

*The Argus Detonations.*—A series of three multi-stage rockets, fired from the *U.S.S. Norton Sound* in the south Atlantic Ocean, delivered small fission bombs to high altitude, where they were detonated. A variety of considerations led to the choice of site for detonations:

(a) An isolated firing area was desired for reasons of safety.

(b) An intermediate latitude was desired in order that the expected lifetime of the trapped particles be at least a few days in order to make possible comprehensive observations. At low latitudes the trapped particles spend a greater fraction of their paths in denser air. And at high latitude, the corresponding magnetic line of force goes farther from the earth in the equatorial plane and a reduction of trapped life time is to be expected due to perturbations in the outer reaches of the geomagnetic field.

(c) It was necessary that the chosen magnetic shell be such that it could be intercepted by a low-altitude satellite in an orbit inclined at not more than 51° to the equatorial plane (the highest inclination which was practical with existing U.S. facilities at that time). An intermediate latitude was preferable to a low latitude, also, because the satellite orbit would then intercept the shell of trapped particles at a less oblique angle.

(d) From the observations of Explorers I and III, it was known that the intensity of the natural radiation diminished rapidly, at a given altitude, as one receded

from the magnetic equator (either north or south). Hence the "background" radiation would be less at intermediate latitudes.

(e) In the south Atlantic, the scalar magnitude of the geomagnetic field is less than that at any other point on the earth at intermediate latitudes. Hence, for a given altitude of injection, the trapped lifetime of charged particles would be the greatest for this firing site (cf. reference 2).

(f) It was desirable that an island or other convenient observing site be located near the point conjugate to the firing point (the Azores Islands, in this case).

In Table 2 are summarized the pertinent data on the three Argus bursts.

TABLE 2  
DATA ON BURSTS

	Argus I	Argus II	Argus III
Nominal yield	1 to 2 kilotons	1 to 2 kilotons	1 to 2 kilotons
Approximate time of burst	August 27, 1958, 0230 U.T.	August 30, 1958, 0320 U.T.	September 6, 1958, 2210 U.T.
Approximate geographic coordinates	38° S, 12° W	50° S, 8° W	50° S, 10° W

Nominal altitude of all bursts—480 km.

*Nature and Scope of Satellite Observations.*—During the month preceding Argus I (July 26 to August 26), an extensive body of observations served to establish the detailed spatial dependence of the natural, trapped radiation and many of its properties in terms of the characteristics of the four detectors which we had devised for the twofold program of observation.

Typical geometric relationships between the orbit of Explorer IV (Satellite 1958 Epsilon) and the chosen magnetic shell are illustrated in a schematic way in Figures 3 and 4. It is seen that in a favorable case the satellite orbit intersects the Argus shell four times during each revolution around the earth—at points A, B, C, and D. These intersections are, of course, at various altitudes, latitudes, and longitudes. In practice the number of observed intersections from which significant data were obtained was much less than four per orbit due to a variety of reasons:

(a) Many of the intersections were at such low altitudes that the intensity of Argus electrons was immeasurably small with the equipment used.

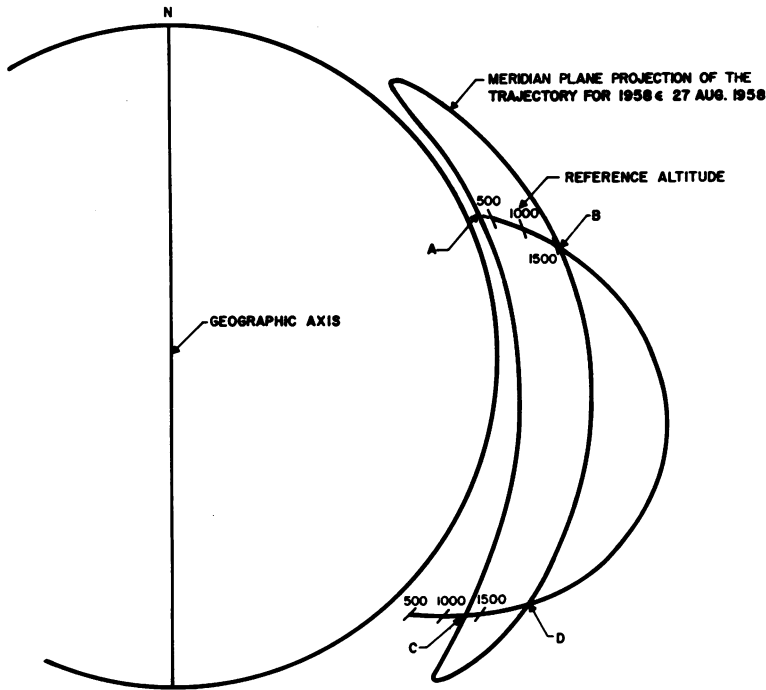
(b) In many cases, fewer than four intersections occurred due to the distortion and tilt of the chosen magnetic shell.

(c) Many intersections occurred beyond radio-telemetry range of any one of the receiving stations.

(d) Some of the intersections occurred at points where the artificially injected radiation was unobservedly small relative to the natural radiation. And, of course, this situation prevailed at all points within the reach of Explorer IV after the lapse of a sufficiently long time.

Table 3 gives a brief tabular summary of the numbers of observed intersections which yielded significant data. It should be noted that the batteries supplying the lower-powered of the two transmitters and telemetry channels 2 and 5 were exhausted on about September 3. The higher-powered transmitter and channels 1, 3, and 4 continued to operate properly until about the 21st of September. At this time the Argus III particles were still being detected above the background on occasional favorable intersections.

It appears probable that a residuum of the Argus electrons was also detected near the geomagnetic equator with Pioneer III on December 6, 1958. But no observable intensity was present there on March 3, 1959 (Pioneer IV).



INTERSECTION OF SATELLITE ORBIT WITH A GEOMAGNETIC SHELL

FIG. 3.—Illustrative diagram showing a sample geometric relationship between the orbit of satellite 1958 epsilon and a chosen magnetic shell at a given longitude.

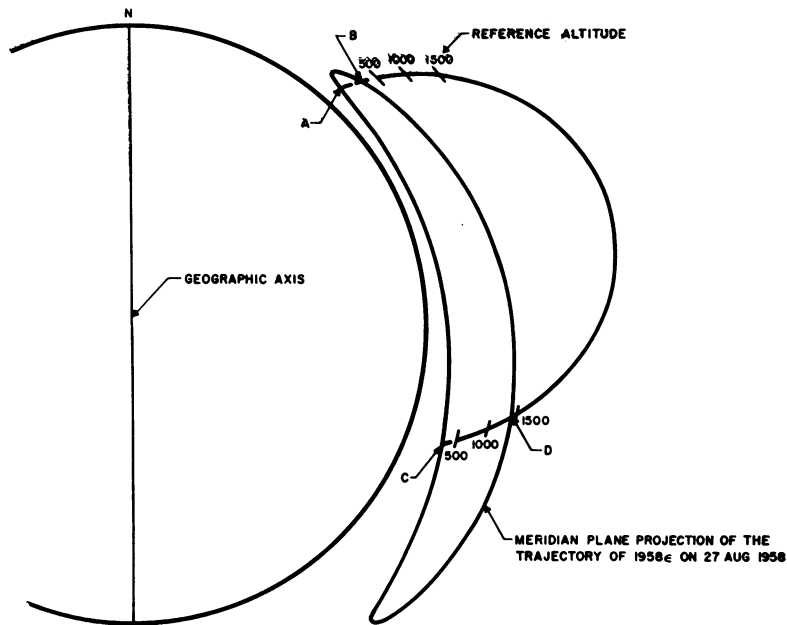
*Detailed Observations.*—The “Argus effect” was easily and promptly observed by Explorer IV after each of the three detonations.

Figure 5 shows a record of measurements of the natural radiation taken on the day before Argus I. Figure 6 shows a record taken on a satellite pass through a similar geographic region about three and one half hours after Argus I. The same data are plotted with a linear scale of ordinates in Figure 7. The great peak which was intersected at 0608 U.T. on August 27 had no precedent in four weeks of previous observations of the natural radiation. Moreover, it was encountered on the first

TABLE 3

SUMMARY OF OBSERVED INTERSECTIONS GIVING SIGNIFICANT DATA

Burst	Number in Northern Hemisphere	Number in Southern Hemisphere	Period of Observations (1958)
Argus I	28	9	August 27 to September 6
Argus II	27	12	August 30 to September 6
Argus III	61	27	September 6 to September 21
Totals	116	48	.....



INTERSECTION OF SATELLITE ORBIT WITH A GEOMAGNETIC SHELL

FIG. 4.—Same as Figure 3, except at a different longitude.

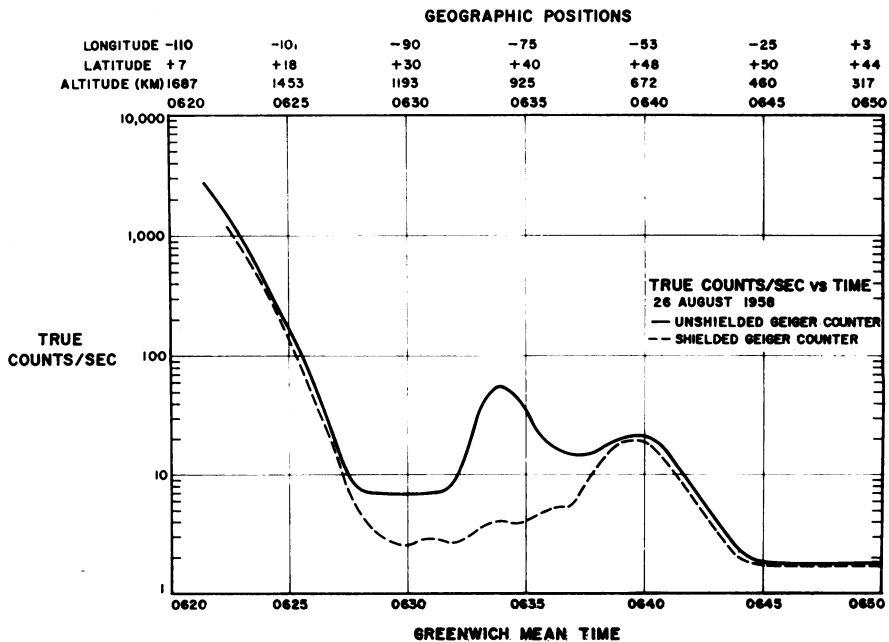


FIG. 5.—A plot of observations of the natural radiation on the day before Argus I.

observed intersection with the planned magnetic shell following the Argus I detonation. Further reasons for the validity of identifying such observed peaks with the "Argus effect" are as follows:

(a) The observed energy spectrum and nature of the radiation were found to be in essential agreement with that expected for the decay electrons from fission fragments.

(b) A peak with similar characteristics was found at every observed intersection of the orbit of the satellite with the appropriate magnetic shell, irrespective of latitude or longitude.

(c) The geometric thickness of the shell was similar to that of pretest estimates.

(d) The observed intensity of trapped electrons was in order-of-magnitude agreement with pretest estimates.

(e) The temporal decay of trapped intensity resembled pretest estimates.

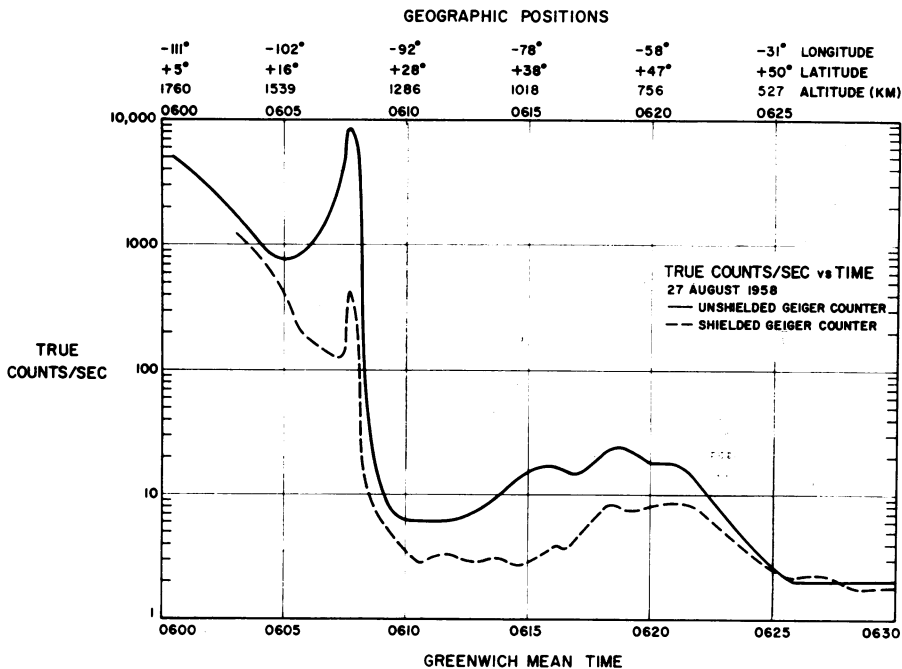


FIG. 6.—A plot of radiation observations showing the Argus I peak at 0608 U.T. on August 27, 1958, about three and one-half hours after the burst. The geographic region is similar to that of Figure 5.

The above remarks apply to the sequences of observations after each of the three shots—Argus I, II, and III. During the entire active period of Explorer IV (July 26 to September 21, 1958), no such peaks were observed except those having the proper temporal and spatial relationship to the artificial ones expected. The observing period included a number of important geophysical perturbations in the radiation around the earth. But these perturbations were of a quite different nature.

Figure 8 is a record on August 31, 1958, which shows the decaying peak due to Argus I (at 0446 U.T.) and the fresh peak due to Argus II (at 0449 U.T.); and Figure 9 is a sample record on September 9, 1958 which shows the peak due to Ar-

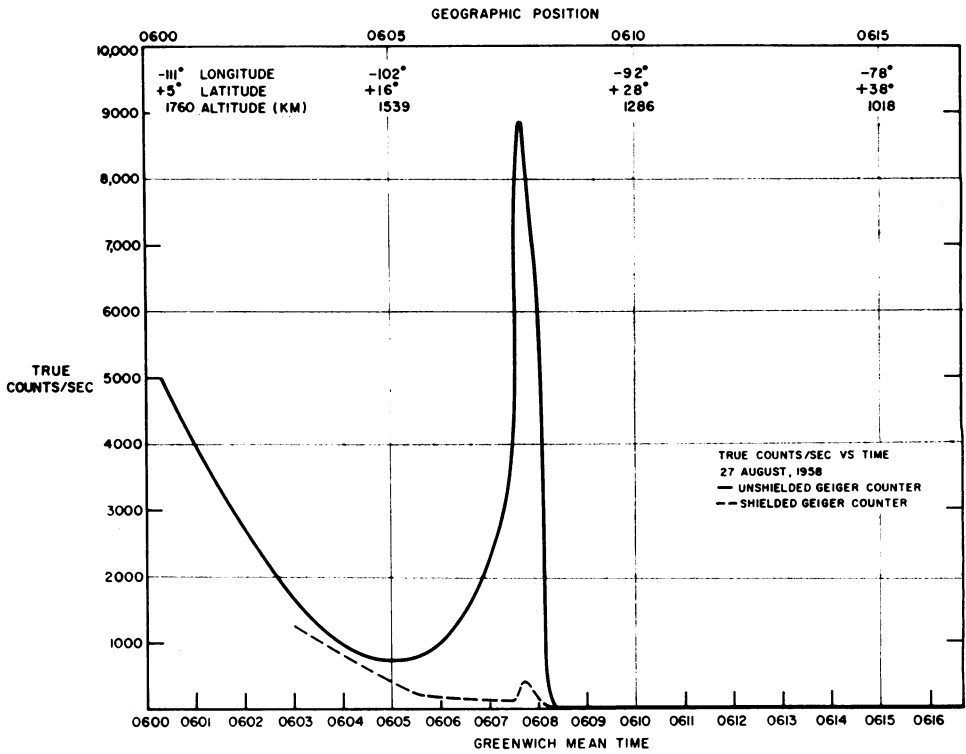


Fig. 7.—Same data as on Figure 6, plotted with a linear scale of ordinates.

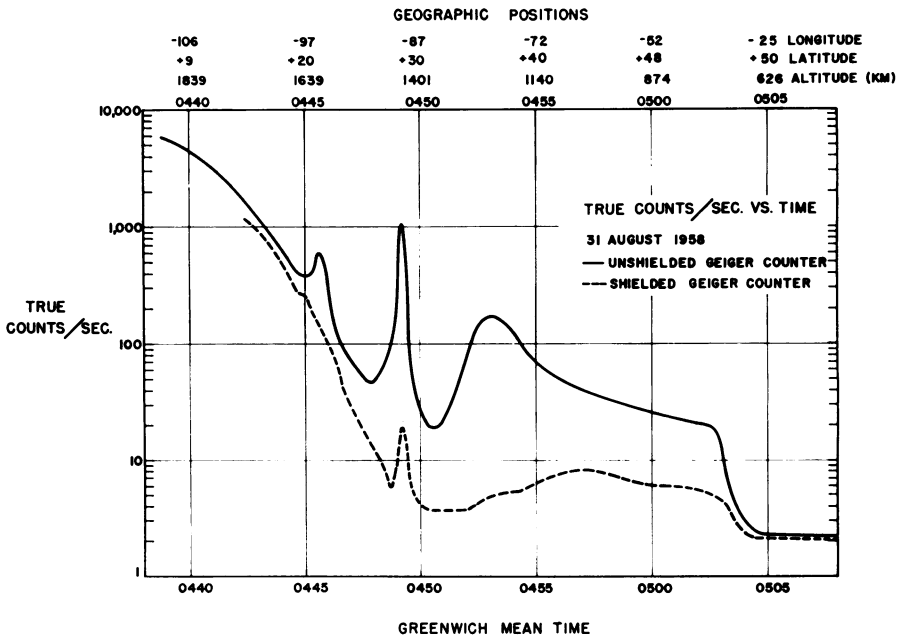


Fig. 8.—A plot of radiation observations on August 31, 1958 showing the decaying Argus I peak (at 0446 U.T.) and the fresh Argus II peak (at 0449 U.T.).

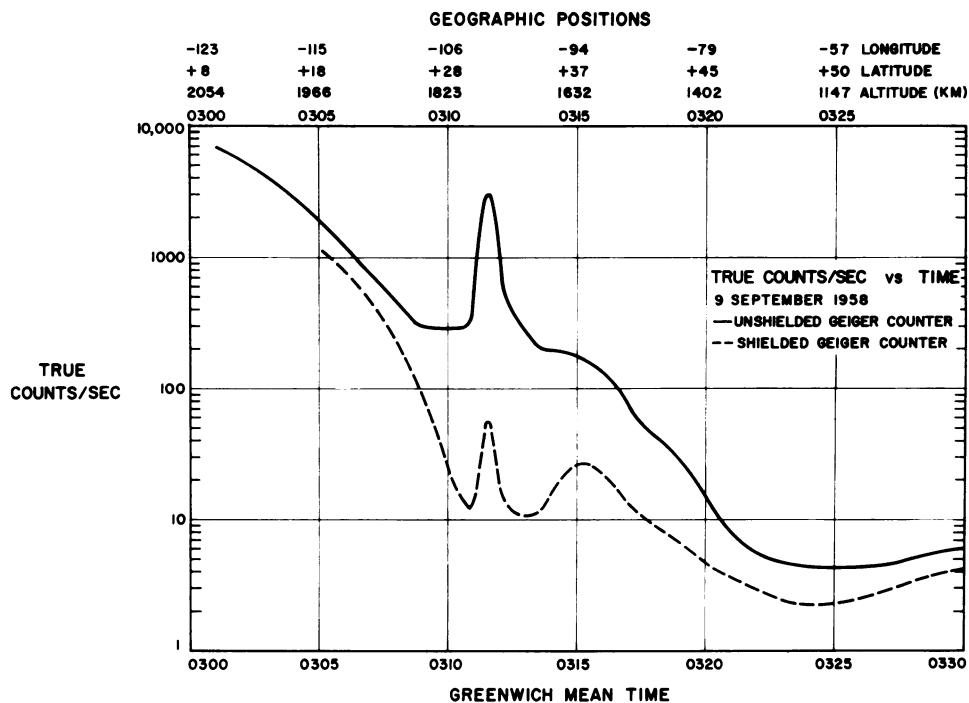


Fig. 9.—A plot of radiation observations on September 9, 1958, showing the Argus III peak at about 0312 U.T.

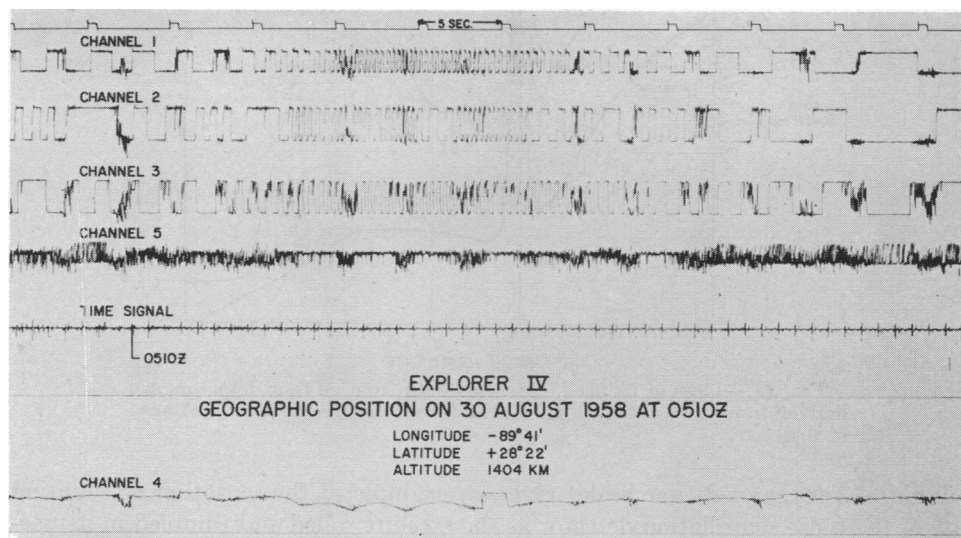


Fig. 10.—Photograph of raw telemetry record (Offner pen-and-ink recorder) of a pass through the Argus II shell on August 30, 1958.

gus III. Figure 10 is a photograph of a raw telemetry record of the passage of Explorer IV through the Argus II shell and Figure 11 gives plots of the reduced, corrected data from all four detectors. These two figures exemplify the data reduction procedure.

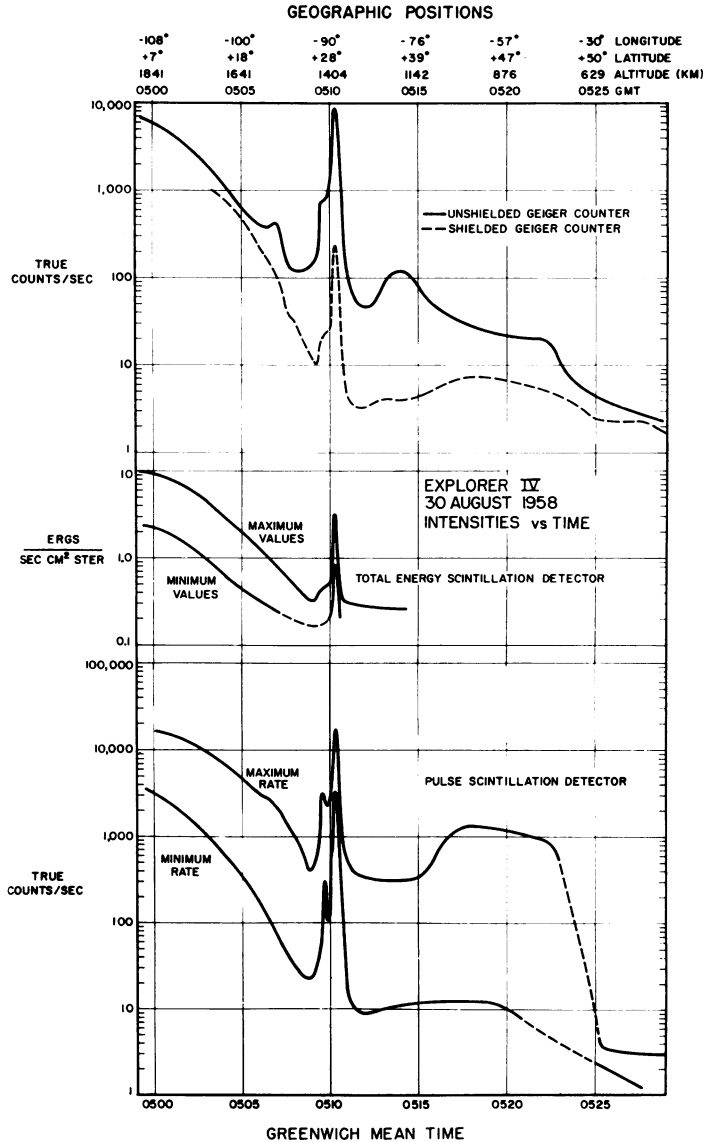


FIG. 11.—Plots of reduced, corrected data from all four detectors as derived from the record of Figure 10 and from the pre-flight calibrations of detectors.

Figure 12 (expanded time scale) gives an example of the variation of counting rate of the pulse scintillation detector as the satellite rolled and tumbled in its passage through the Argus I shell. As previously described<sup>2</sup> this type of "random" angular motion is very advantageous for the measurement of angular distributions. The angular distributions of the Argus electrons (as observed near their mirror altitudes) were found to be disklike in nature, as suggested by magnetic-trapping theory and as extensively observed on the natural radiation.

In each set of observations (cf. Figures 10 and 11), the output of each detector

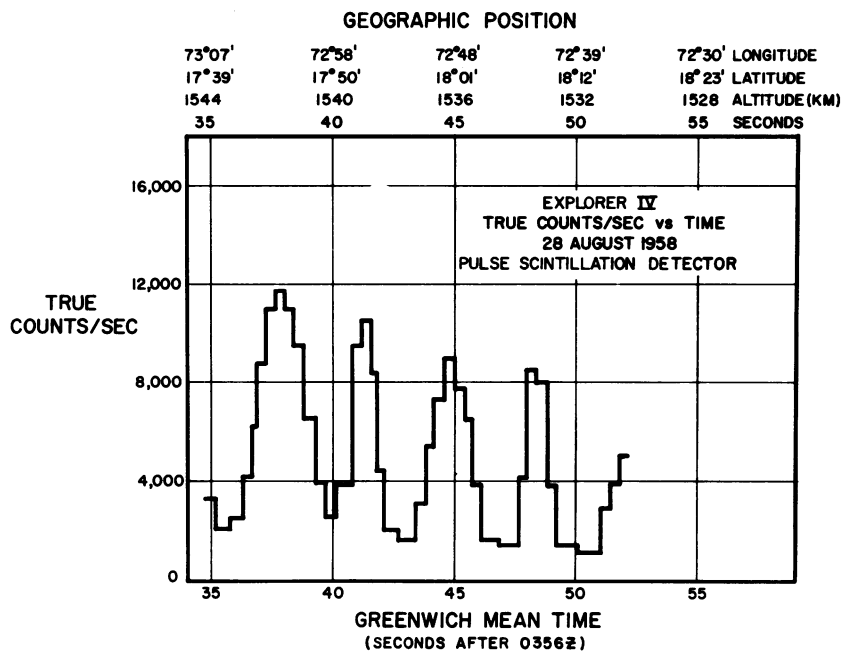


FIG. 12.—A plot on an expanded time scale of the detailed counting rate of the pulse scintillation counter as a function of time during passage through the Argus I shell. This plot illustrates the disk-like angular distribution of the radiation. The tumble period was 7 seconds.

was converted either to true counting rate (channels 1, 2, 3, and 5) or to absolute directional energy flux (channel 4) using preflight calibration data; and from the corrected plots the following quantities were estimated:

- (a) Net intensity above background of observed Argus electrons, obtained by subtraction of the interpolated background values.
- (b) The time width of the Argus peak at half-maximum intensity.
- (c) The time width of the Argus peak at one-tenth maximum intensity.
- (d) The local maximum and minimum values of intensity near the center of the peak.
- (e) The time at which the center of the peak occurred. Then, from the ephemeris of the satellite<sup>2</sup> the following were tabulated:
- (f) Geographic location (latitude, longitude, and altitude) of the center of the observed peak.
- (g) Geometric thickness of the "shell" of electrons at half-maximum intensity, measured perpendicular to the shell.

*Organization and Analysis of Observations.*—The work sketched in the present section was considerably advanced by a ten-day study session arranged and conducted by the Department of Defense during February, 1959, at the Lawrence Radiation Laboratories in Livermore, California. The group specifically concerned with satellite observations consisted of the following persons: George Bing (Chairman), Donald Chandler, Rolf Dyce, William Karzas, John Killeen, Charles Lundquist, Hans Mark, Carl McIlwain, Paul Nakada, Theodore Northrup, Ralph Pennington, Russell Shelton, James Van Allen, and Ernest Vestine.

As mentioned earlier, the various observations occurred at a great variety of positions in space. And, of course, the irregular nature of the geomagnetic field produces essential complications. The foundations for organizing the data are indicated in Figure 13. By the basic Poincare-Stoermer-Alfven theory of the trapping

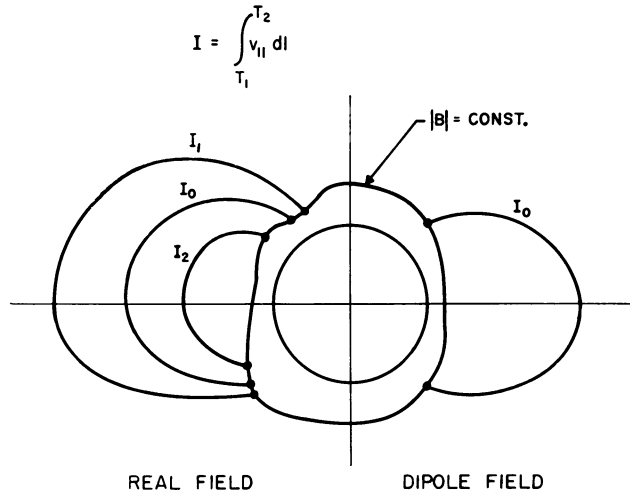


FIG. 13.—A diagram to illustrate the principles of conservation of  $\mu$  and  $I$  in geomagnetic trapping. (See text.)

of charged particles in the geomagnetic field the magnetic moment of a spiraling particle is an adiabatic invariant of the motion. That is

$$\mu = \frac{1/2 m v_{\perp}^2}{B} = \text{constant}$$

Since the speed  $v$  (having components  $v_{\parallel}$  and  $v_{\perp}$  at any moment parallel and perpendicular, respectively, to the magnetic vector  $B$ ) is also a constant of the motion in a static magnetic field, the turning points (or mirror points) of the oscillatory, helical path of a given particle always occur at the same scalar value,  $B$ . Indeed, the locus of the turning points of all particles of given magnetic moment is a surface of  $B = \text{constant}$  (cf. Figure 13).

Also, as first conjectured by Rosenbluth and Longmire<sup>3</sup> and later discussed in detail by others, the line integral along a line of force between turning points for a given particle:

$$I = \int_{\tau_1}^{\tau_2} v_{\parallel} dl = v \int_{\tau_1}^{\tau_2} \sqrt{1 - B/B_r} dl$$

is an adiabatic invariant (under an important class of physical conditions) of its motion, where  $B_r$  is the scalar value of  $B$  at the turning points  $\tau_1$  and  $\tau_2$ .

This latter principle makes possible the identification of a unique sequence of magnetic lines of force which constitute a single valued, three-dimensional surface on which the guiding center of the particle will forever lie—to the extent that the conditions for the conservation of  $\mu$  and  $I$  are met—as it moves about in the irregular geomagnetic field. The argument is illustrated in Figure 13. Let the surface  $B = \text{const.}$  shown there represent the locus of turning points for a particle having a given

magnetic moment  $\mu$ . Let the particle's motion, at a chosen period of time, be along the line of force shown in the right-hand side of the figure with the integral  $I$  having the value  $I_0$ . The question then is: Along which of the infinite number of segments of lines of force having values of  $I-I_0, I_1, I_2$ , etc. (sketched in the left-hand side of Figure 13)—and having turning points on the specified surface of constant  $B$  will the guiding center of the particle's trajectory be moving at some later time? The Rosenbluth principle assures one that it will be the segment characterized by  $I_0$ , or more precisely by  $I_0/v$ .

To the extent that the above discussion is applicable to electrons having energies up to several million electron volts and trapped in the real geomagnetic field it may be expected that an Argus shell of trapped electrons will maintain its integrity and will be fixed with respect to the earth.

Moreover, elementary consideration of perturbations by localized magnetic irregularities and by atmospheric scattering and energy-loss indicates that the tendency for diffusion of guiding centers transverse to the shell will be greatly exceeded by the tendency for diffusion of turning points along the shell and that the latter tendency will result in progressive leakage of particles downward into the denser atmosphere and eventual loss.

Hence, the temporal decay of the total number of trapped particles resulting from an impulsive injection may be expected to proceed by way of loss of particles out of the ends of the shell; and it may be further expected that the geometric thickness and position of the shell with respect to the earth will be substantially constant.

In the first instance, the observations following each detonation are functions of four apparently independent parameters—latitude, longitude, altitude, and elapsed time from the time of the detonation.

The considerations of the preceding paragraphs (which have been most clearly advocated by T. Northrup and implemented by E. H. Vestine) suggest that important progress can be made in systematizing the observations for the purpose of interpretation if the three positional parameters, latitude, longitude, and altitude, be supplanted by a single one—the scalar value  $B$  at the position of the observation. Apart from perturbations whose effects are important during one longitudinal precession period (order of a fraction of an hour in the present case), a surface of constant  $B$  may be expected, at a given time, to be a surface of constant particle intensity irrespective of the distorted shape of this surface in the real geomagnetic field.

Hence, it may be hoped that observable features of the trapped Argus radiation will be functions of only two parameters,  $B$  and elapsed time.

The geomagnetic field has a slow secular rate of change and  $B$  is not accurately known as a function of geographic coordinates during August–September, 1958. In the present work Vestine and associates have derived pertinent  $B$  values from the recent British 48-coefficient potential function (era of 1955). Small errors also arise from the imperfect knowledge of the orbit of the satellite ( $\pm 10$  km) and from the observational uncertainty in locating the center of the shell of electrons.

*Preliminary Summary of Significance of Observations.*—(1) *Thickness of Argus shells:* The observed mean thickness of the Argus shells at half-intensity, measured perpendicular to the boundaries of the shells, was about 90 km for events I and II and 150 km for event III. The thickness of the shells did *not* have a systematic dependence on elapsed time, but the scatter of the measured values of thickness is of the

order of 30 per cent and no lesser broadening (or thinning) of the shell during the observing period could be discerned. It is presumed that the basic shell thickness was determined by the very complex injection situation at and immediately after the detonation in each case. This surmise is supported by crude consideration of the dynamics of the detonation in the earth's magnetic field.

It does seem to be of importance that the leakage of particles from the shell (by energy loss and "longitudinal" diffusion) proceeded at a sufficiently rapid rate that the transverse diffusion was, in general, unobservably small. (See, however, a later section remarking on the influence of the geomagnetic storm of September 3 ff.) And it may be noted that the magnetic shell in question reaches outward to a radial distance of about two earth radii from the center of the earth.

These results, of course, provide a quantitative validation of the principle of conservation of  $I$  in the geomagnetic field.

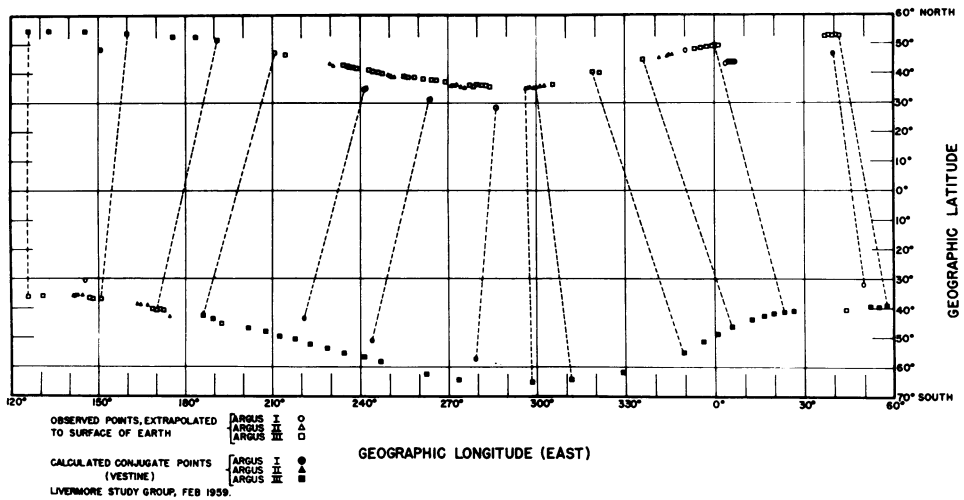


FIG. 14.—Plot of (extrapolated) observed intersections of Argus shells' I, II and III with surface of the earth, and computed conjugate points (after Vestine and Pennington). (Livermore study group.)

(2) *Position of the shell in space:* Each observation of the center of each Argus shell (I, II, and III) was projected down to the surface of the solid earth by use of a simplified model of the geomagnetic field, the eccentric dipole model. A comprehensive plot of the results of this process is shown in Figure 14, together with conjugate points calculated with the full 48-coefficient potential function. The three resulting loci of points, interlaced in time, are notably smooth and regular suggesting the positional stability of the several shells during the observing period. A more critical examination of this question can be had by examination of Figure 15, a large scale plot of projected observations on Argus III. In view of the interlacing of observations at various sequences of times, we conclude that the shell could not have drifted monotonically in latitude by more than about  $0.03^\circ$  of latitude per day (about 2 km of distance per day at 1500 km) without having resulted in an unreasonable "ripple" in the implied geomagnetic field contour.

These results are in the nature of a confirmation both qualitatively and quantitatively of the principles which have been sketched in preceding sections.

(3) *Angular distribution:* As typified by Figure 12 (see also reference 2), the angular distribution of the trapped electrons was always observed to be disklike in character with an angular thickness of the order of  $\pm 20^\circ$  or less. In terms of the basic dynamics of the trapping of charged particles this fact shows that, at the relatively low altitudes of observation, most particles being measured have their turning points not more than a few hundred kilometers below the observing point—a quite reasonable result.

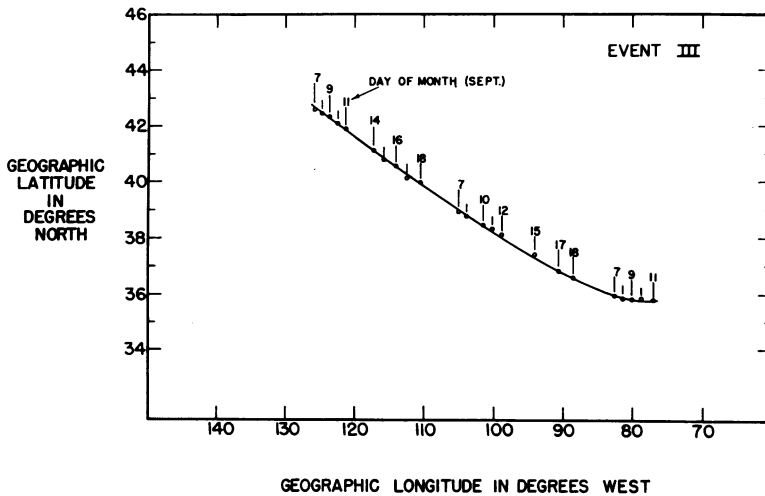


FIG. 15.—An expanded plot of a portion of Figure 14.

(4) *Trapped lifetimes:* The product of the maximum observed intensity,  $C$ , at the center of the shell times the thickness,  $W$ , of the shell at half-intensity has been taken as a measure of the total intensity of trapped particles (within the detection range of the detector in question). Several preliminary plots of this quantity,  $CW$ , versus elapsed time,  $t$ , for two different ranges of  $B$  are given in Figures 16, 17 and 18. The plots are of data from channel 3 (the unshielded Geiger tube). Closer examination of several selected cases suggests that the scatter of data will be reduced by taking proper account of the average aspect of the satellite equipment as it passed through the shells. It is seen that  $CW$  varies approximately as the negative first power of the elapsed time. This law of time-decay of trapped intensity, namely  $CWt = \text{const.}$  is in general accord with a theory of the loss mechanism due to Ernest C. Ray of this laboratory (to be published). The above curves based on our channel 3 data (the most extensive and simple body of data) pertain to an effective electron energy of about 3.5 mev. By comparison with the theory Ray finds that the effective atmospheric density at 1,000 km required to reduce the intensity as rapidly as observed is at least 10 times as great as one would suppose from the plausible extrapolation of the Jastrow "satellite-drag" atmosphere.

It is of interest to note that the Argus shells occurred (Fig. 19) within the "slot"

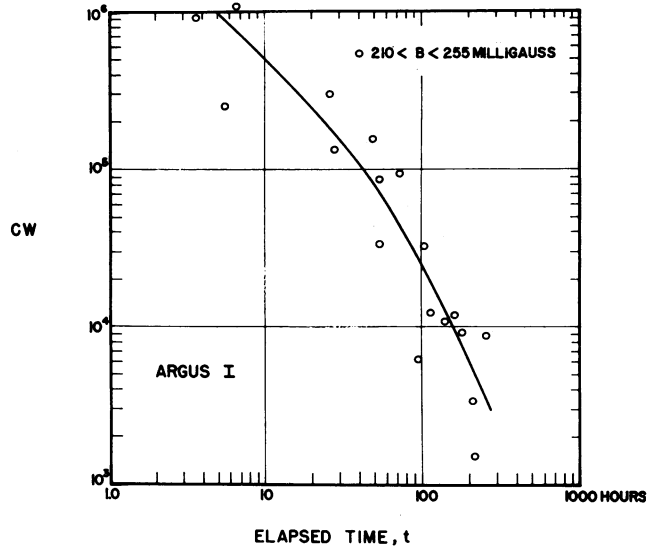


FIG. 16.—The product of maximum true counting rate,  $C$ , of channel 3 at center of Argus I shell times the geometric width (thickness) at half-maximum,  $W$ , versus elapsed time,  $t$ . (Livermore Study Group.)

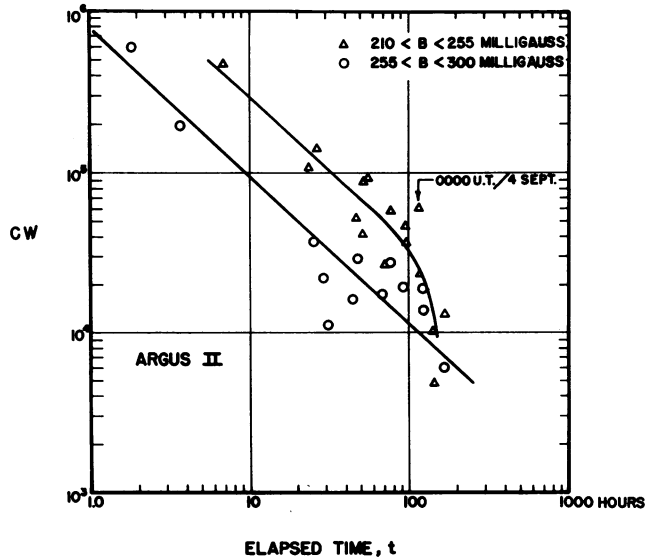


FIG. 17.—The product of maximum true counting rate,  $C$ , of channel 3 at center of Argus II shell times the geometric width (thickness) at half-maximum,  $W$ , versus elapsed time,  $t$ . (Livermore Study Group.)

between the two natural radiation zones.<sup>4, 5</sup> It may be that the atmospheric density is anomalously high there.

An alternative line of speculation would suppose that the rapid decay was, at least in part, due to "magnetic diffusion" due to small scale and perhaps time-de-

pendent irregularities of the geomagnetic field. A more conclusive discussion of this point is in process, making use of the results from all four detectors (different effective particle energies).

The gross decay rate is presumably a composite of atmospheric and magnetic effects.

The present experimental results on artificially injected electrons are of far reaching importance in understanding the dynamics of the natural radiation.

The discontinuously rapid drop of intensity of Argus I and Argus II on about the 4th of September suggests that the great magnetic storm of that date may have caused a greatly enhanced rate of loss of stored particles. Also, the thickness of the Argus II shell appears to have increased significantly during the same period.

These observations may provide an important clue to the understanding of the structure and intensity of the natural radiation belts.

(5) *Injection efficiency:* By means of our Explorer IV observations, it is possible

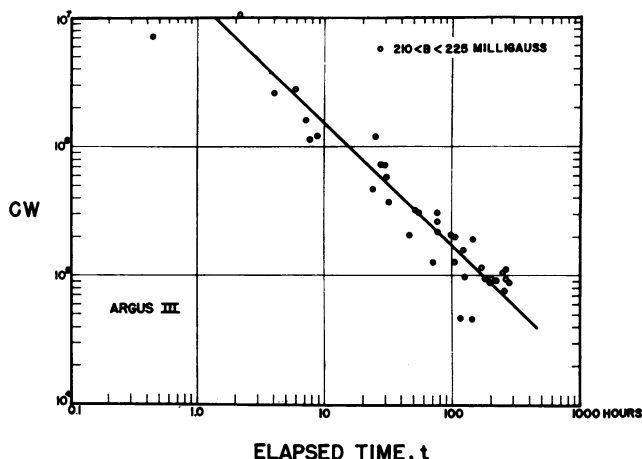


FIG. 18.—The product of maximum true counting rate,  $C$ , of channel 3 at center of Argus III shell times the geometric width (thickness) at half-maximum,  $W$ , versus elapsed time,  $t$ . (Livermore Study Group.)

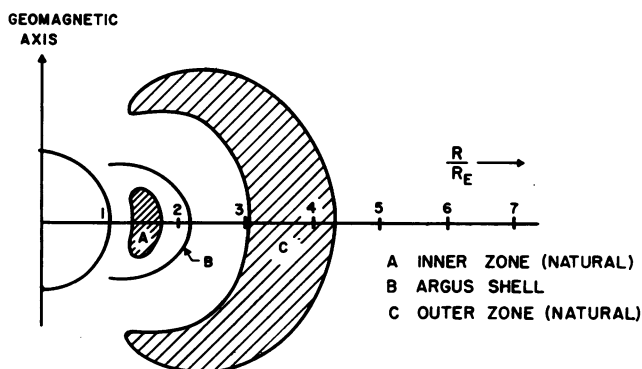


FIG. 19.—The general relationship of the Argus shells to the structure of the natural radiation zones. See references 4 and 5.

to estimate the total number of trapped Argus electrons having turning points below the highest altitude of observation. This estimate, made as of zero elapsed time, serves to place a lower limit on the fraction of electrons effectively injected into the geomagnetic field, since the nominal yield and nominal spectrum of electrons are known.

(6) *Distribution of turning points:* Figure 20 is a plot of  $CWt$  versus  $B$  for Argus I, II, and III. The distribution of turning points along a line of force is implicit in these curves. It is seen that there is a monotonic increase in the density of turning points with decreasing  $B$  (increasing altitude). It is therefore evident that injection of the longer-lived electrons occurred, in large part, at altitudes much greater than that of the atomic detonations.

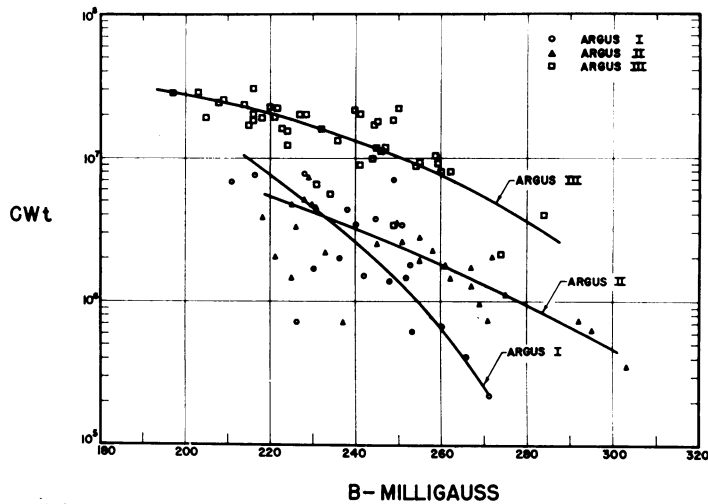


FIG. 20.—The triple product of  $C$  times  $W$  times  $t$  for channel 3 versus scaler magnetic field intensity  $B$  for Argus I, Argus II and Argus III. (Livermore Study Group.)

(7) *The general geomagnetic field:* The geometric form of the Argus shells is known to a precision of the order of  $\pm 10$  km with respect to the earth. Hence, these experiments provide a significant new method for the harmonic analysis of the general geomagnetic field. This analysis is not yet completed but it is already clear that at least the dipole and quadrupole terms will be determined with useful accuracy.

The Argus work at the State University of Iowa has been supported, in large part, by contract no. DA-11-022-ORD-2788 with the Chicago Ordnance District of the Department of the Army, which support is gratefully acknowledged.

<sup>1</sup> Van Allen, J. A., G. H. Ludwig, E. C. Ray, and C. E. McIlwain, "Observation of High Intensity Radiation by Satellites 1958 Alpha and Gamma," *Jet Propulsion*, **28**, 588-592 (1958).

<sup>2</sup> Van Allen, J. A., C. E. McIlwain, and G. H. Ludwig, "Radiation Observations with Satellite 1958 $\epsilon$ ," *Journal of Geophysical Research*, **64**, 271-286 (1959).

<sup>3</sup> Rosenbluth, M. N., and C. L. Longmire, "Stability of Plasmas Confined by Magnetic Fields,"

*Annals of Physics*, 1, 120-140 (1957). (Apparently the first paper on the matter in the open literature.)

<sup>4</sup> Van Allen, J. A., and L. A. Frank, "Radiation Around the Earth to a Radial Distance of 107,400 km," *Nature*, 183, 430-434 (1959).

<sup>5</sup> Vernov, S. N., A. Ye. Chudakov, P. V. Vakulov, and Yu. I. Logachev, "Study of Terrestrial Corpuscular Radiation and Cosmic Rays During Flight of the Cosmic Rocket," *Doklady Akademii Nauk S.S.S.R.*, 125, 304-307 (1959).

---

### PROJECT JASON MEASUREMENT OF TRAPPED ELECTRONS FROM A NUCLEAR DEVICE BY SOUNDING ROCKETS

BY LEW ALLEN, JR., JAMES L. BEAVERS II, WILLIAM A. WHITAKER,  
JASPER A. WELCH, JR., AND RODDY B. WALTON

PHYSICS DIVISION, RESEARCH DIRECTORATE, AIR FORCE SPECIAL WEAPONS CENTER, AIR RESEARCH AND DEVELOPMENT COMMAND, KIRTLAND AIR FORCE BASE, NEW MEXICO

*Equipment.*— Project Jason is the name for the Air Force Special Weapons Center's participation in the Argus experiment. It consisted of the firing of 19 high-altitude sounding rockets to measure the electrons created by the Argus detonations. The carrier vehicle used was a five-stage solid propellant rocket consisting of an Honest John for the first stage, Nike boosters for the second and third stages, a Recruit for the fourth stage, and a T-55 for the fifth stage. These were capable of delivering a 50-pound payload to an altitude of 800 km when launched at an elevation of 80°. They were launched from three sites: Cape Canaveral, Florida (Air Force Missile Test Center); Wallops Island, Virginia (NASA Pilotless Aircraft Test Station); and Ramey Air Force Base, Puerto Rico. Table 1 gives some particulars of each launching. The flights are referred to by Patrick Air Force Base test number and are listed in chronological, rather than numerical, order. The table shows the launch site, date of launch, launch time after the appropriate burst, and the apogee and splash coordinates of the flight. Also shown are the rocket spin and tumble periods.

The instrumentation used in this project was basically a radiation sensing system composed of eight Geiger-Müller tubes and a system for providing a data link to ground receiving. Inasmuch as new phenomena were being investigated, it was necessary to provide a radiation detecting system with various thresholds and dynamic ranges that would best satisfy the expected conditions. Several tubes were collimated to observe the angular distribution of the electron flux. The selected values for thresholds and dynamic ranges proved quite adequate. In the design of the instrumentation system, effort was made to provide a system with a minimum number of components and maximum reliability. The package was designed and constructed under contract by Lockheed MSD; Figure 1 shows a breakdown of the complete instrumentation package. The transducer head, some aspects of which are shown schematically in Figure 2, consisted of eight G-M tubes arranged around the circumference of the forward portion of the instrumentation package. The tubes were protected during the lower atmospheric portion of the flight by a nose cap which was jettisoned at an altitude of 400,000 feet, approximately. After jettison of nose cap, all the detector circuitry became